BIOCHEMISTRY

 Volume 46, Number 22 June 5, 2007

Articles

FTIR Study on the Hydrogen Bond Structure of a Key Tyrosine Residue in the Flavin-Binding Blue Light Sensor TePixD from *Thermosynechococcus elongatus*†

Ryouta Takahashi,‡ Koji Okajima,§ Hiroyuki Suzuki,‡ Hiro Nakamura,||,⊥ Masahiko Ikeuchi,§ and Takumi Noguchi*,‡

Institute of Materials Science, University of Tsukuba, Tsukuba, Ibaraki 305-8573, Japan, Department of Life Sciences (Biology), The University of Tokyo, Komaba, Meguro, Tokyo 153-8902, Japan, RIKEN Harima Institute/SPring-8, Mikazuki, Sayo, Hyogo 679-5148, Japan, and International Graduate School of Arts and Sciences, Yokohama City University, Suehiro, Tsurumi, Yokohama, Kanagawa 230-0045, Japan

Received March 7, 2007; Revised Manuscript Received April 9, 2007

ABSTRACT: The BLUF (sensor of blue light using FAD) domain is a blue light receptor possessing a flavin molecule as an active cofactor. A conserved Tyr residue located adjacent to flavin has been proposed to be a key amino acid in the mechanism of the photoreaction of the BLUF domain. We have studied the structure of this key Tyr residue and the relevance to the photoreaction in the BLUF protein of the cyanobacterium *Thermosynechococcus elongatus*, TePixD, by means of Fourier transform infrared (FTIR) difference spectroscopy and density functional theory (DFT) calculations. Light-induced FTIR difference spectra of unlabeled and [4-^{13}C]Tyr-labeled TePixD in H_2O and D_2O revealed that the νCO/δCOH vibrations of a photosensitive Tyr side chain are located at 1265/1242 cm^{-1} in the dark-adapted state and at 1273/1235 cm^{-1} in the light-induced signaling state. These signals were assigned to the vibrations of Tyr8 near flavin from the absence of the effect of [4-^{13}C]Tyr labeling in the Tyr8Phe mutant. DFT calculations of H-bonded complexes of *p*-cresol with amides as models of the Tyr8−Gln50 interactions showed that Tyr8 acts as a H-bond donor to the Gln50 in both of the dark and light states. Further DFT analysis suggested that this H-bond is strengthened upon photoconversion to the light state accompanied with a change in the H-bond angle. The change in the H-bond structure of Tyr8 is coupled to the flavin photoreaction probably through the Tyr8−Gln50−flavin H-bond network, suggesting a significant role of Tyr8 in the photoreaction mechanism of TePixD.

Light sensing is an important process in most of living things. To date, three types of blue light sensor domains using flavin as an active cofactor are known: LOV (light oxygen voltage) in phototropins, PHR (photolyase homology region) in cryptochromes, and BLUF[1] (sensor of blue light using FAD) (*1*, *2*). The BLUF domain is involved in a wide range of bacterial and eukaryotic proteins (*2*) such as AppA (*3*, *4*) and BlrB (*5*) in the photosynthetic bacterium *Rhodobacter*

† This study was supported by Grants-in-Aid for Scientific Research (17GS0314 and 18570145 to T.N. and 17657013, 16370018, and 16087102 to M.I.) from the Ministry of Education, Science, Sports, Culture, and Technology.

* To whom correspondence should be addressed. Phone: +81-29-853-5126. Fax: +81-29-853-4490. E-mail: tnoguchi@ims.tsukuba.ac.jp.

‡ University of Tsukuba.

§ The University of Tokyo.

|| RIKEN.

⊥ Yokohama City University.

[1] Abbreviations: FTIR, Fourier transform infrared; BLUF, sensors of blue light using FAD; νCO, CO stretching vibration; δCOH, COH bending vibration; FAD, flavin adenine dinucleotide; DFT, density functional theory.

10.1021/bi7004653 CCC: $37.00
Published on Web 05/12/2007

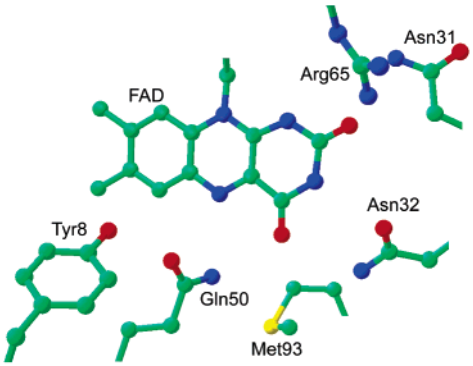

FIGURE 1: X-ray structure of the FAD binding site of TePixD (*22*).

sphaeroides, PixD (positive phototaxis factor D) in cyanobacteria (*6*, *7*) [SyPixD (or Slr1694) from *Synechocystis* PCC6803; TePixD (or Tll0078) from *Thermosynechococcus elongatus*], PAC in the green alga *Euglena gracilis* (*8*), and YcgF from *Escherichia coli* (*9*). They regulate a variety of functions, e.g., controlling photosynthesis gene expression by AppA (*4*), photophobic movement of cells by PAC (*8*), and photophobic regulation of pili-dependent cell motility by SyPixD (*6*).

Signal transduction in BLUF proteins is initiated by blue light absorption by flavin and subsequent conversion from the dark-adapted state (dark state) to the light-induced signaling state (light state). This photoconversion is characterized by an ~10 nm red shift of flavin electronic absorption (*4*, *6*, *10*−*13*) and a large downshift of the νC4═O frequency of flavin (*7*, *10*, *14*−*21*). The light state has a relatively long lifetime (seconds to minutes) and slowly relaxes to the dark state. The changes in BLUF domain structures upon light-state formation triggers subsequent reactions such as dissociation of PpsR from AppA (*4*), that of PixE from SyPixD (*6*, *7*), and activation of the adenylyl cyclase domain in PAC (*8*), which are involved in signal transduction cascades.

The X-ray crystallographic structures of BLUF domains have recently been reported for TePixD (*22*), SyPixD (*23*), AppA (*24*, *25*), and BlrB (*5*) at 1.8−2.3 Å resolutions. Figure 1 shows the crystal structure of the flavin binding site of TePixD (*22*). The flavin isoalloxazine ring is surrounded by several polar amino acids, forming H-bond networks. The Tyr residue in the vicinity of flavin is conserved among BLUF domains (*2*), and mutagenesis studies showed that this Tyr is indispensable for the proper photoreactions (*7*, *10*, *12*, *15*, *26*, *27*). In TePixD, Tyr8Ala and Tyr8Phe mutants lost the normal red-shifting photoreaction and instead showed reduction of a flavin following its triplet-state formation (*7*). In SyPixD, AppA, and PAC, mutations at the corresponding Tyr residue inactivated the photoreaction (*10*, *12*, *15*, *26*, *27*). Thus, the Tyr interacting with flavin through the Tyr−Gln−flavin H-bond network must be crucial in the photoreaction mechanism of the BLUF domains.

The recent time-resolved absorption study by Gauden et al. (*28*) resolved the transient intermediates in the photoreaction of SyPixD as a FAD anion radical ($FAD^{\bullet -}$) and a subsequently formed neutral radical ($FADH^{\bullet}$). They proposed that oxidation of nearby Tyr by the excited singlet-state FAD* and subsequent formation of a $Tyr^{\bullet}-FADH^{\bullet}$ radical pair are essential mechanisms of the BLUF reaction. This radical pair formation triggers a switching of the Tyr−Gln−FAD H-bond network by an ~180° flip of the Gln side chain. As a result, the H-bond at FAD N5 is shifted to that at C4═O, and the H-bond form of Tyr is changed from a H-bond acceptor [TyrO(H)···H_2N] to a H-bond donor (TyrOH···O═C) (*28*). A similar mechanism of electron transfer from Tyr to flavin triggering subsequent H-bond rearrangement was also proposed in a time-resolved study of AppA by Dragnea et al. (*27*). The flipping of Gln during photoreaction has been proposed in studies of AppA BLUF (*14*, *24*, *25*, *29*) and SyPixD (*23*). Thus, in the above model of the photoreaction mechanism, Tyr plays a key role in both the electron transfer and subsequent H-bond switching.

To understand the molecular mechanism of the photoreaction of PixD, determination of the H-bond structure of the Tyr8 is essential. However, the X-ray structure (*5*, *22*−*25*) did not answer this problem clearly because of the difficulty in detecting hydrogen atoms and discriminating between nitrogen and oxygen atoms in amide groups. In this study, the H-bond structure of the Tyr8 in TePixD and its change upon photoreaction were investigated using light-induced FTIR difference spectroscopy, which is a powerful method to identify the protonation and H-bond structures of proteins and cofactors in active sites. We have assigned the νCO and δCOH vibrations of a Tyr side chain using selective labeling of Tyr residues with [4-^{13}C]Tyr. In addition, [4-^{13}C]Tyr labeling of the site-directed Tyr8Phe mutant was performed to identify the signals of Tyr8. The band frequencies were analyzed by density functional theory (DFT) calculations for H-bond complexes of *p*-cresol with amides as models of the Tyr−Gln interactions. The results showed that Tyr8 acts as a H-bond donor in both the dark and light states, and its H-bond strength and angle are perturbed by the photoreaction.

MATERIALS AND METHODS

The N-terminal $(His)_6$-tagged TePixD of *T. elongatus* BP-1 was expressed with pET28a vectors in *E. coli* BL21(DE3), and cells were grown in the LB medium containing 20 μg/mL kanamycin for 12 h at 37 °C (*7*). Site-directed mutagenesis of TePixD was performed using the PCR-based QuickChange site-directed mutagenesis kit (Stratagene, La Jolla, CA) (*7*). [4-^{13}C]Tyr-labeled TePixD was expressed in the tyrosine auxotroph, *E. coli* BL21(DE3)Y, which was constructed by P1 transduction as previously described (*30*). In this case, cells were grown in 1 L of modified medium containing 0.1 g of L-[4-^{13}C]Tyr in the presence of 19 other unlabeled L-amino acids (*30*). TePixD was purified by nickel-affinity column chromatography with elution buffer (pH 7.5) containing 20 mM Hepes, 1 M NaCl, and 500 mM imidazole (*22*).

For preparation of FTIR samples, TePixD in the elution buffer was diluted by a factor of 10, and the aggregated protein was collected by centrifugation. The protein was washed with 10 mM Hepes−NaOH buffer (pH 7.5) and resuspended in the same buffer to result in a concentration of ~5.0 mg of protein/mL. For preparation of deuterated samples, TePixD was dissolved in 0.5 M Hepes−NaOD/D_2O buffer (pD 7.5) containing 1 M NaCl and 0.5 M imidazole and incubated for 24 h at 4 °C. The deuterated TePixD was then collected by centrifugation after dilution with D_2O and resuspended in 10 mM Hepes−NaOD/D_2O

buffer (pH 7.5). An aliquot of the sample suspension (6 μL) was dried on a CaF_2 plate (25 mm in diameter) under N_2 gas flow to make a film in an elliptical shape (6 mm × 9 mm) and was sealed with another CaF_2 plate with a greased Teflon spacer (0.5 mm in thickness). The dry film was hydrated (or deuterated) by placing 2 μL of 20% (v/v) glycerol/H_2O [or glycerol$(OD)_3$/D_2O] in a sealed infrared cell without touching the sample (*31*). The sample temperature was adjusted to 10 °C by circulating cold water in a copper holder.

Light-induced FTIR spectra were measured using a Bruker IFS-66/S spectrophotometer equipped with an MCT detector (Infrared D316/8) at 4 cm^{-1} resolution. Single-beam spectra were recorded for 50 s before and during illumination by white light (~18 mW/cm^2 at the sample surface) from a halogen lamp (Sigma Koki PHL-150). The measurement was repeated six times with an interval of 20 min, and a light minus dark difference spectrum was generated using averaged single-beam spectra. Spectral fitting was performed using the IGOR Pro program (Wavemetrics Inc.).

MO calculations were performed using the Gaussian03 program package (*32*). The B3LYP functional (*33*, *34*) with the 6-31+G(d,p) basis set was used to optimize the geometry of the model complexes and calculate the vibrational frequencies. Calculated frequencies were scaled with a single scaling factor of 0.977 to adjust the calculated νCO frequency of free *p*-cresol to the experimental value of 1255 cm^{-1} (*35*).

RESULTS

Figure 2a (black line) shows a light-induced FTIR difference spectrum of unlabeled TePixD, which represents the structural changes upon the conversion from the dark-adapted state to the light-induced signaling state. Overall spectral features were similar to those of other BLUF domains such as SyPixD (*15*, *16*, *18*), AppA (*10*, *19*, *20*), and YcgF (*17*). In particular, the prominent negative/positive peaks were observed at 1713/1698 cm^{-1}, which have been assigned to the νC4═O vibration of flavin (*7*, *10*, *14*−*21*). The large downshift of the νC4═O frequency was attributed to the decrease in the force constant of the C4═O bond due to a stronger H-bond interaction in the light state (*14*−*21*). Other peaks at 1700−1600 cm^{-1} have been mainly attributed to the amide I bands (C═O stretch of backbone amides) and νC2═O, while peaks at 1600−1500 cm^{-1} have been mainly assigned to the amide II bands (NH bend coupled to the CN stretch of backbone amides) and the CN stretching vibrations of a flavin isoalloxazine ring (*17*−*19*). In addition to these vibrations, bands of amino acid side groups whose structures are perturbed by the photoreaction should be involved in the difference spectrum.

To identify the bands of Tyr, especially, vibrations involving a phenolic OH group, substitution of Tyr side chains with [4-^{13}C]Tyr, in which the carbon atom bearing the OH group is labeled with ^{13}C (Figure 2, inset), was performed, and a light-induced FTIR difference spectrum was recorded (Figure 2a, red line). The spectrum was superimposed on the unlabeled one after normalization at the 1713/1698 cm^{-1} signal. Appreciable spectral changes were observed in the regions of 1520−1500 and 1300−1200 cm^{-1}. The negative peak at 1512 cm^{-1} downshifted to 1510 cm^{-1}, and the features at 1273(+)/1261(−)/1248(−)/1233-

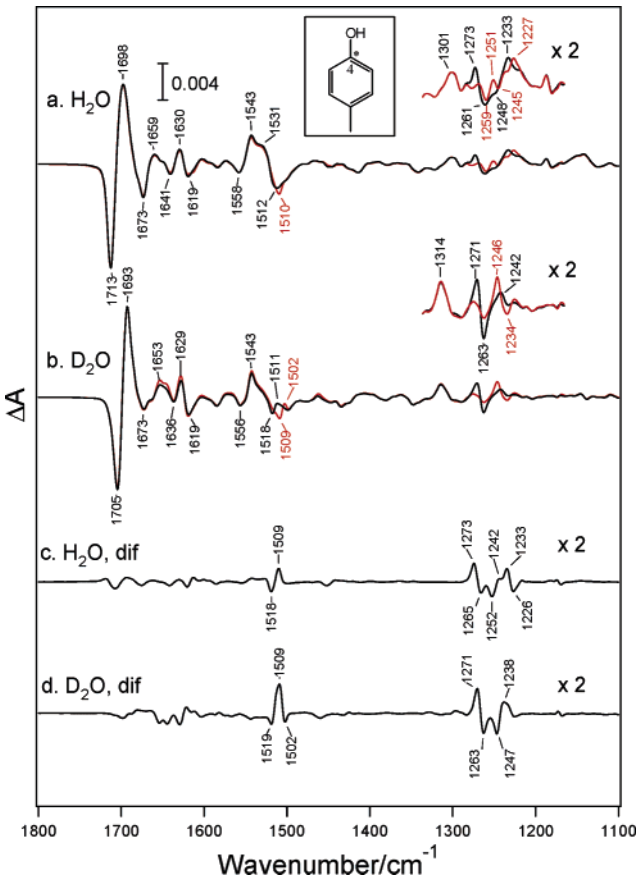

FIGURE 2: (a, b) Light-induced FTIR difference spectra of unlabeled (black line) and [4-^{13}C]Tyr-labeled (red line) TePixD in H_2O (a) and D_2O (b). (c, d) Double difference spectra between the [4-^{13}C]-Tyr-labeled and unlabeled spectra (unlabeled minus [4-^{13}C]Tyr-labeled) in H_2O (c) and D_2O (d). The inset shows the position of the carbon atom labeled with ^{13}C (indicated by *) in a Tyr side chain.

(+) cm^{-1} were changed to those at 1259(−)/1251(+)/1245-(−)/1227(+) cm^{-1}. These isotope-induced changes were better expressed in the double difference spectrum (unlabeled minus [4-^{13}C]Tyr-labeled) (Figure 2c), which was calculated using the spectra normalized to the 1713/1698 cm^{-1} intensity (Figure 2a). A differential signal at 1518(−)/1509(+) cm^{-1} and a rather complex feature with peaks at 1273(+)/1265-(−)/1252(−)/1242(+)/1233(+)/1226(−) cm^{-1} were observed. It is noted that small signals at 1720−1600 cm^{-1} probably originate from subtle changes in the amide I and νC4═O bands due to a slight difference in sample conditions. These bands have been reported to be sensitive to hydration extent and temperatures in FTIR spectra of SyPixD (*16*). Indeed, a double difference spectrum between light-induced spectra obtained using different samples of unlabeled TePixD showed small changes in the same region with intensities comparable to those in Figure 2c. It should be emphasized, however, that the noise level of the 1300−1200 cm^{-1} region in this double difference spectrum of unlabeled TePixD was much lower than the signals at 1280−1220 cm^{-1} in Figure 2c (the ratio of maximum peak-to-peak intensities was less than 0.07).

Thus, the bands at 1520−1500 and 1300−1200 cm^{-1} in the double difference spectrum arise from the Tyr vibrations involving the carbon-4 atom in the phenyl ring. The former and latter frequency regions are typical of the νCC and νCO/δCOH vibrations, respectively, of a Tyr side chain (*36*−

40). Changes in the similar region by [4-^{13}C]Tyr labeling have been observed in Tyr in aqueous solution and the redox-active Tyr in photosystem II (*39*, *40*). For assignments of the νCO and δCOH bands showing close frequencies in the 1300−1200 cm^{-1} region, light-induced FTIR spectra were recorded in D_2O (Figure 2b). Upon deuteration of the OH group of Tyr, the δCOD frequency significantly downshifts to <1000 cm^{-1} (*36*); hence, the δCOH bands disappear, and only the νCO bands remain in the 1300−1200 cm^{-1} region. Indeed, the spectrum showed a simpler feature with peaks at 1271(+)/1263(−) cm^{-1} (Figure 2b, black line), which downshifted to 1246(+)/1234(−) cm^{-1} upon [4-^{13}C]Tyr labeling (Figure 2b, red line). The double difference spectrum (Figure 2d) also showed a simpler shape with four major peaks at 1271(+)/1263(−)/1247(−)/1238(+) cm^{-1}, indicating that δCOH bands disappeared and only the νCO bands were left as expected. Note that weak intensities at 1233 and 1226 cm^{-1} remained in the double difference spectrum (Figure 2d) due to undeuterated Tyr partially left in the sample.

In the νCC region of the double difference spectrum in D_2O, three peaks were observed at 1519(−)/1509(+)/1502(−) cm^{-1} with a strongest intensity in the 1509 cm^{-1} peak (Figure 2d). This band shape was different from that in H_2O, which showed two peaks at 1518(−)/1509(+) cm^{-1} with nearly equivalent intensities (Figure 2c). These band shapes may indicate that a differential signal at 1519/~1509 cm^{-1} in D_2O and a signal at 1518 cm^{-1} in H_2O downshifted by ~10 cm^{-1} upon [4-^{13}C]Tyr labeling. Our DFT calculations showed that the νCC vibration is slightly coupled with the δCOH vibration when COH is H-bonded (not shown), which may be the cause of the different behavior of νCC bands between the spectra in H_2O and D_2O.

The νCO/δCOH (in H_2O) or νCO (in D_2O) signals of Tyr in the double difference spectra were decomposed with Gaussian bands assuming that the spectrum in H_2O consists of four νCO bands (ν^{12}CO and ν^{13}CO of the dark and light states) and four δCOH bands (δ^{12}COH and δ^{13}COH of the dark and light states) (Figure 3A) and that in D_2O (after subtraction of the residual undeuterated component) consists of four νCO bands (ν^{12}CO and ν^{13}CO of the dark and light states) (Figure 3B). Each spectrum was successfully decomposed with the expected number of Gaussian bands, indicating that only a single Tyr side chain in TePixD was affected by the photoreaction. The obtained peak frequencies and shifts upon isotope labeling are summarized in Table 1. In the dark state, the νCO and δCOH vibrations are found at 1265 and 1242 cm^{-1}, respectively, and in the light state, the νCO frequency upshifts to 1273 cm^{-1} by 8 cm^{-1} whereas the δCOH frequency downshifts to 1235 cm^{-1} by 7 cm^{-1}. In deuterated TePixD, the νCO bands in the dark and light states appear at 1262 and 1270 cm^{-1}, respectively. The slightly lower (by 3 cm^{-1}) frequencies than those in undeuterated TePixD are attributed to decoupling of the δCOH vibration mixed in the νCO normal mode. Identification of the δCOH bands also provides solid evidence that the photosensitive Tyr in TePixD does not take a tyrosinate form (Tyr-O$^-$) but takes a protonated form (Tyr-OH) in both the dark and light states.

The best candidate for the Tyr residue observed in the FTIR spectra is Tyr8 that interacts with flavin through a H-bond network (Figure 1) (*22*). To confirm the origin of the Tyr signals, the spectrum of the Tyr8Phe mutant, in which Tyr8 was replaced with Phe, was recorded, and the effect of [4-^{13}C]Tyr labeling was examined. The spectrum of the unlabeled Tyr8Phe mutant (Figure 4a, black line) showed

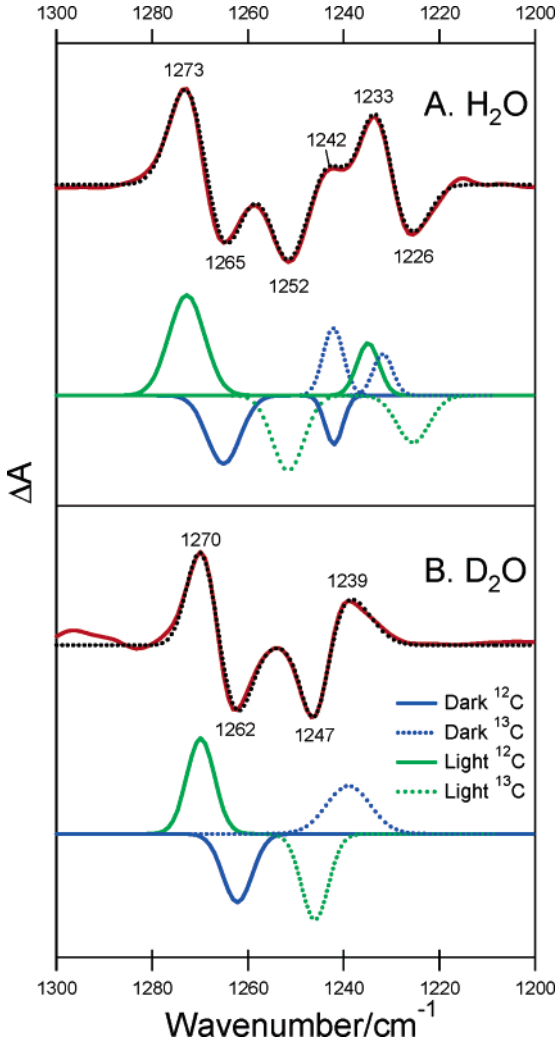

FIGURE 3: Tyr νCO/δCOH region in the isotope-induced double difference spectra [unlabeled minus ([4-^{13}C]Tyr-labeled)] (red lines) in H_2O (A) and D_2O (B) and deconvolution of the spectra with Gaussian bands (blue and green lines). The experimental spectrum in D_2O (B, red line) is a corrected spectrum after removing the contribution of undeuterated portion. Spectral fitting was performed by fixing the positions of rather isolated peaks at 1273, 1265, 1252, and 1226 cm^{-1} in (A) and of all four peaks in (B). Blue and green lines indicate the bands in the dark and light states, respectively, and solid and dotted lines indicate the bands of unlabeled (^{12}C-Tyr) and 4-^{13}C-labeled Tyr, respectively. The sum of the Gaussian bands (black dotted line) is overlaid on the experimental spectrum.

Table 1: Frequencies (cm^{-1}) of the νCO and δCOH Vibrations of Photosensitve Tyr in the Dark and Light States of TePixD

	νCO		δCOH	
	^{12}C-Tyr	[4-^{13}C]Tyr (Δ)[a]	^{12}C-Tyr	[4-^{13}C]Tyr (Δ)[a]
in H_2O				
dark state	1265	1242 (−23)	1242	1232 (−10)
light state	1273	1252 (−21)	1235	1226 (−9)
in D_2O				
dark state	1262 (−3)[b]	1239 (−23)		
light state	1270 (−3)[b]	1247 (−23)		

[a] Values in parentheses are frequency shifts by [4-^{13}C]Tyr labeling. [b] Values in parentheses are frequency shifts by deuteration.

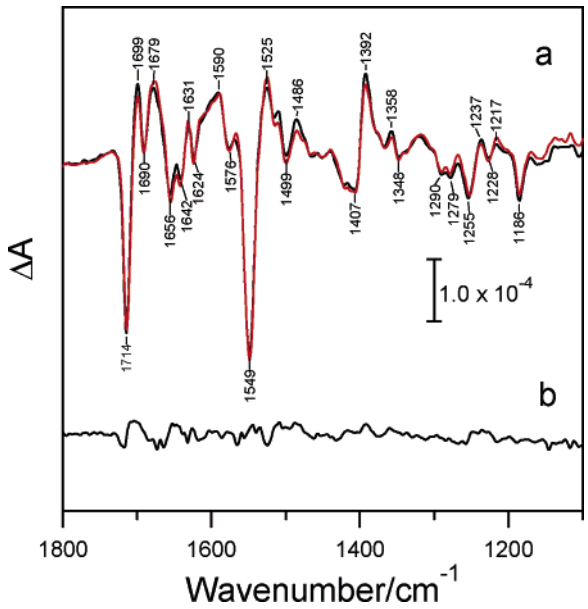

FIGURE 4: (a) Light-induced FTIR difference spectra of the Tyr8Phe mutant of TePixD. Black line: unlabeled TePixD. Red line: [4-^{13}C]-Tyr-labeled TePixD. (b) Double difference spectrum between the [4-^{13}C]Tyr-labeled and unlabeled spectra (unlabeled minus [4-^{13}C]-Tyr-labeled) of the Tyr8Phe mutant.

features significantly different from those of the wild-type spectrum (Figure 2a). A number of strong or medium peaks were newly observed at 1680−1000 cm^{-1}, in addition to the 1714/1699 cm^{-1} peaks, which most probably correspond to the νC4═O peaks at 1713/1698 cm^{-1} in the wild-type spectrum. The strongest signal was a negative peak at 1549 cm^{-1}. A prominent signal around 1550 cm^{-1} along with strong or medium peaks at 1500−1000 cm^{-1} is similar to the feature of light-induced FTIR spectra of LOV domains (*41*, *42*) and cryptochrome (*43*), suggesting that the chemical structure of the flavin isoalloxazine ring was somehow modified rather than simple H-bond changes as proposed for the BLUF domains. This observation is consistent with the previous proposal that the Tyr8Phe mutant of TePixD undergoes flavin reduction (*7*). The FTIR spectrum of the [4-^{13}C]Tyr-labeled sample of Tyr8Phe is shown in Figure 4a (red line) superimposing that of the unlabeled mutant sample (black line). Both spectra were basically identical, and no specific difference was observed. This was more clearly shown in the double difference spectrum (Figure 4b), showing no specific bands in the Tyr νCO/δCOH region. It is noted that the higher noise level in the spectra of the Tyr8Phe mutant (Figure 4) than that of the wild type (Figure 2) is ascribed to a lower efficiency of photoreaction in the mutant and hence to the smaller signal intensities (by a factor of ∼50).

To identify the H-bond structure of the Tyr in TePixD from the observed νCO/δCOH frequencies, vibrational frequencies of model complexes of Tyr with different forms of H-bond interactions were calculated using the DFT method. We used H-bonded complexes of *p*-cresol with acetamide as models of H-bonding interactions of Tyr with a Gln side chain. *p*-Cresol has been used as a model of a Tyr side chain in FTIR and Raman investigations of Tyr interactions (*36*−*40*). Although we used acetamide as a H-bond partner, the purpose of this calculation is not exact reproduction of the Tyr−Gln interaction in TePixD but

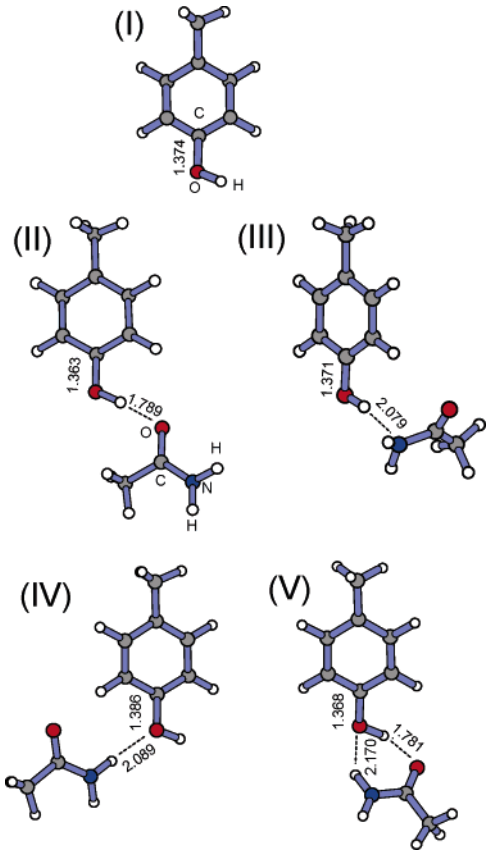

FIGURE 5: Optimized structures of *p*-cresol (I) and its H-bonded complexes (II−V) with acetamide as models of the Tyr8−Gln50 interaction in TePixD: (I) free *p*-cresol; (II) *p*-cresol as a H-bond donor to the oxygen atom of amide; (III) *p*-cresol as a H-bond donor to the nitrogen atom of amide; (IV) *p*-cresol as a H-bond acceptor; (V) *p*-cresol as both a H-bond donor and an acceptor.

examining the general effects of H-bonding on the νCO/δCOH frequencies. Thus, the mutual arrangement of *p*-cresol and acetamide does not necessarily agree with that in the X-ray structure of TePixD. Figure 5 shows the optimized structures of free *p*-cresol (I) and its H-bonded complexes with acetamide, in which *p*-cresol acts as a H-bond donor to the oxygen atom (II) or the nitrogen atom (III) of amide, as a H-bond acceptor (IV), and as both H-bond donor and acceptor (V). All of the calculated frequencies were scaled with a single scaling factor of 0.977 to adjust the CO frequency of free *p*-cresol to the experimental value (1255 cm^{-1}) (*35*). Calculated νCO and δCOH frequencies are summarized in Table 2 together with shifts by deuteration of the OH group and by 4-^{13}C labeling. When *p*-cresol acts as a H-bond donor to the amide C═O (model II), the νCO frequency showed an upshift by 19 cm^{-1} from that of free *p*-cresol resulting in the frequency of 1274 cm^{-1}, and the δCOH vibration also exhibited a significant upshift of 84 cm^{-1} to give a frequency of 1240 cm^{-1}. A similar tendency of shifts was observed when *p*-cresol is H-bonded to the nitrogen atom of amide (model III), but upshifts were much smaller, i.e., +6 and +53 cm^{-1} for νCO and δCOH, respectively, due to a rather weak H-bond as shown in the H-bond distances (2.079 Å in model III in comparison with 1.789 Å in model II; Figure 5). On the other hand, when *p*-cresol acts as a H-bond acceptor (model IV), a relatively large downshift of the νCO frequency by −23 cm^{-1} was observed to give a frequency of 1232 cm^{-1}, and the δCOH

Table 2: Calculated Frequencies (cm^{-1}) of the νCO and δCOH Vibrations of *p*-Cresol and Its H-Bonded Complexes with Acetamide

H-bond form (structure in Figure 5)[a]	νCO			δCOH		
	frequency[b] (ΔH-bond)[c]	ΔD[d]	Δ4-^{13}C[e]	frequency[b] (ΔH-bond)[c]	ΔD[d]	Δ4-^{13}C[e]
free *p*-cresol (I)	1255 (0)	−6	−25	1156 (0)	−255	−4
OH···O=C (II)	1274 (+19)	−10	−21	1240 (+84)	−246	−16
OH···NH_2 (III)	1261 (+6)	−10	−23	1209 (+53)	−264	−16
O(H)···H_2N (IV)	1232 (−23)	−3	−22	1167 (+11)	−255	−3
OH···O=C/O(H)···H_2N (V)	1241[f] (−14)	+15	−17	1241[f] (+85)	−267	−17

[a] The optimized structure of each complex is shown in Figure 5. [b] Calculated frequencies were scaled with a factor of 0.977 to adjust the νCO frequency of free *p*-cresol to the experimental value (*35*). [c] Shifts by H-bond formation. [d] Shifts upon deuteration of the OH group. [e] Shifts upon 4-^{13}C labeling. [f] The mode in which the νCO and δCOH vibrations are strongly coupled with each other.

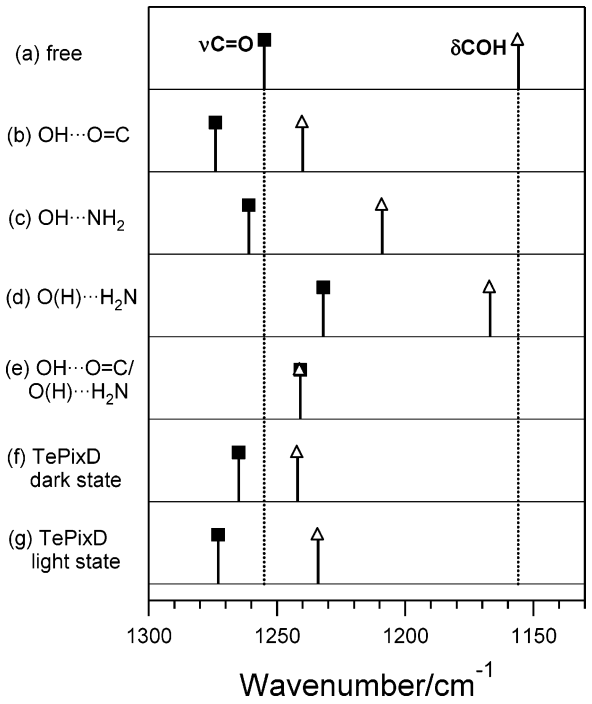

FIGURE 6: Calculated frequencies of the νCO (closed squares) and δCOH (open triangles) vibrations of *p*-cresol in model complexes with different H-bond forms in comparison with the experimental frequencies of Tyr8 in TePixD in the dark and light states.

was calculated to be 1167 cm^{-1} as a result of a medium upshift by 11 cm^{-1}. Finally, when both of the hydrogen and oxygen atoms of the OH are H-bonded simultaneously (model V), the νCO downshifted and the δCOH significantly upshifted, and as a result, these vibrations were strongly coupled with each other to form a mode with a strong infrared intensity at 1241 cm^{-1}. We have calculated the νCO and δCOH frequencies of *p*-cresol with various H-bonding partners other than amides (Takahashi and Noguchi, unpublished results) and found that the above tendencies of νCO and δCOH shifts depending on the H-bond forms generally hold. These calculated results are also in good agreement with experimental data of *p*-cresol or Tyr in various solvents and crystal forms (*37*, *38*). Takeuchi et al. (*37*) showed that νCO occurs at 1275−1265 cm^{-1} in H-bond donating states and at 1240−1230 cm^{-1} in H-bond accepting states, while Gerothanassis et al. (*38*) reported a large increase in the δCOH frequency by H-bond formation as a donor or as both donor and acceptor. Thus, νCO and δCOH can be good markers to determine the H-bond forms of a Tyr side chain.

In Figure 6, the experimental νCO and δCOH frequencies of the photosensitive Tyr in TePixD in the dark and light states are compared with the calculated frequencies with different H-bond forms. In both states, the νCO frequencies (1265 and 1273 cm^{-1} in the dark and light states, respectively) are located above the free νCO frequency, and the δCOH frequencies (1242 and 1235 cm^{-1} in the dark and light states, respectively) are found at significantly higher positions than the δCOH frequency of free *p*-cresol (Figure 6f,g). This experimental νCO/δCOH pattern is in good agreement with the pattern of a H-bond donor (Figure 6b,c) but significantly differs from that of a H-bond acceptor (Figure 6d). The structure of double H-bonds (Figure 6e) is also dismissed, because in this structure the νCO and δCOH vibrations are strongly coupled with each other showing a frequency slightly lower than the free νCO. Thus, the H-bond donor is the most probable H-bond form of the photosensitive Tyr in both the dark and light states of TePixD. As a H-bond partner, the amide C=O is in better agreement with the experimental data than the nitrogen of amide NH_2. In the structures as a H-bond donor, shifts of the νCO/δCOH frequencies by 4-^{13}C labeling were calculated to be −23 to −21/−16 cm^{-1} (Table 2), in fair agreement with the experimental values of −23/−10 and −21/−9 cm^{-1} in the dark and light states, respectively (Table 1).

Table 3: Calculated νCO and δCOH Frequencies (cm^{-1}) of *p*-Cresol in H-Bonded Complexes with Various Amides in Which *p*-Cresol Acts as a H-Bond Donor to Amide C=O

amide (H-bond acceptor)[a]	H-bond distance (Å)[b]	νCO[c]	δCOH[c]
formamide	1.820	1273	1231
acetamide	1.789	1275	1240
N-methylformamide	1.800	1274	1237[d]
N-methylacetamide	1.783	1276	1243[d]
diformamide	1.899	1266	1222
N,*N*-dimethylformamide	1.789	1275	1239[d]
N-formylacetamide	1.862	1268	1224[d]

[a] The optimized structures of model complexes are shown in Figure S1 other than the complex with acetamide (Figure 5, model II). [b] The H-bond distance between the hydrogen atom of *p*-cresol OH and the oxygen atom of amide C=O [*r*(H···O)]. [c] Calculated frequencies were scaled with a factor of 0.977. [d] Frequencies decoupled with amide vibrations by isotope substitution of the amide group.

To further study the structural implication of the changes in the νCO/δCOH frequencies upon photoconversion, vibrational frequencies were calculated for model complexes of *p*-cresol H-bonded with various amides. In these complexes, *p*-cresol acts as a H-bond donor to amide C=O. The calculated νCO and δCOH frequencies together with the H-bond distances are summarized in Table 3, and the optimized structures of these complexes other than the complex with acetamide (Figure 5, model II) are shown in

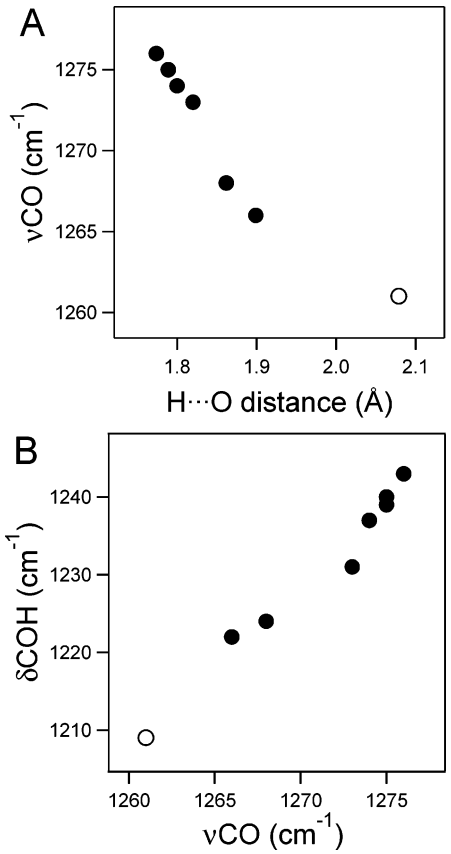

FIGURE 7: (A) Correlation between the H-bond distance and the νCO frequency of *p*-cresol calculated for the model complexes of *p*-cresol H-bonded with various amides. In the complexes, the OH group of *p*-cresol acts as a H-bond donor to amide C═O (solid circles) or to the nitrogen of acetamide (open circle). (B) Correlation between the calculated νCO and δCOH frequencies of *p*-cresol in model H-bonded complexes (solid circles, H-bond to C═O of various amides; open circle, H-bond to the nitrogen of acetamide).

Figure S1 (see Supporting Information). Figure 7A (solid circles) shows that the νCO frequency is well correlated to the H-bond distance; a shorter H-bond distance (i.e., a stronger H-bond) gives a higher νCO frequency. This correlation also holds for the model with a weak H-bond to the amide nitrogen (open circle; Figure 5, model III). When this correlation is applied to the experimental data of TePixD, which showed an 8 cm^{-1} upshift of the νCO frequency upon photoconversion (Table 1), it is concluded that the H-bond of Tyr8 is strengthened by the formation of the light state.

Calculation of the model complexes also shows the correlation of the δCOH frequency with the νCO frequency (Figure 7B). Complexes with higher νCO also have higher δCOH frequencies. This relationship is contrary to the shift direction of the δCOH in TePixD, i.e., a downshift by 7 cm^{-1} upon photoconversion (Table 1). Since the δCOH frequency should be directly affected by the COH angle, the photoconversion of TePixD may induce the changes not only in the H-bond strength of Tyr but also in its H-bond angle.

DISCUSSION

FTIR measurements of TePixD in which Tyr residues are selectively labeled with [4-^{13}C]Tyr showed that signals from a Tyr side chain are involved in the light-induced FTIR difference spectrum upon transition from the dark state to the light-signaling state (Figure 2). This observation indicates that there is a Tyr residue that is coupled to the photoreaction of the flavin in TePixD and this Tyr undergoes some structural changes by the formation of the light state. Spectral analysis by measurements in D_2O and band fitting in the νCO/δCOH region of 1300−1200 cm^{-1} (Figure 3) showed that only a single Tyr side chain is related to these signals and the νCO/δCOH frequencies were identified to be 1265/1242 cm^{-1} in the dark state and 1273/1235 cm^{-1} in the light state (Table 1).

TePixD contains six Tyr residues (Tyr8, Tyr18, Tyr43, Tyr63, Tyr113, and Tyr137) (*22*). Among them only Tyr8 is conserved in different BLUF domains (*2*). Tyr8 is also located in close vicinity of the flavin isoalloxazine ring (Figure 1); in the X-ray structure of TePixD, the distance from the oxygen atom of the Tyr8 side chain to the nearest edge of the ring is 3.3 Å, whereas the other five Tyr residues are located more than 10 Å apart from the isoalloxazine ring. The Tyr8Phe mutant exhibited an FTIR spectrum (Figure 4) significantly different from the wild-type spectrum, probably reflecting photoreduction of the isoalloxazine ring (*7*). Interestingly, the Tyr8Phe mutant of SyPixD did not show any light-induced reactions (*15*), indicative of some difference between TePixD and SyPixD. The presence of the 1714/1699 cm^{-1} peaks (Figure 4) also suggests that the H-bond change at C4═O similar to the wild-type reaction takes place in addition to the flavin change. Thus, amino acid residues structurally coupled to the flavin through H-bond networks are expected to be perturbed by the photoreaction of the Tyr8Phe mutant, although the nature of perturbation could be different from that of the wild type. [4-^{13}C]Tyr labeling of TePixD from the Tyr8Phe mutant, however, did not show any difference from the unlabeled spectrum (Figure 4), indicating that Tyr signals are not involved in the Tyr8Phe spectrum. These results strongly support the assignment of the Tyr bands in the wild-type spectrum to Tyr8, whose structure is perturbed by formation of the light state.

Analysis of the νCO/δCOH frequencies of Tyr8 (Table 1) using DFT calculations for different H-bond forms of the *p*-cresol−acetamide complex (Figure 5, Table 2) as a model of Tyr8−Gln50 interaction showed that Tyr8 in both the dark and light states takes basically the same H-bond form as a H-bond donor (Figure 6). In both states, the νCO/δCOH pattern is more consistent with the structure H-bonded to the oxygen atom than to the nitrogen atom of an amide group (Figure 6). This is because H-bonding to the nitrogen of the amide is much weaker than that to C═O as shown in the longer H-bond distance (1.789 and 2.079 Å for H···O and H···N, respectively; Figure 5). This H-bond structure as a donor to the amide C═O is in agreement with the X-ray structure of TePixD (Figure 1) (*22*). In the X-ray structure of SyPixD by Yuan et al. (*23*), however, a few subunits out of ten took a different conformation, in which the amide nitrogen is directed to Tyr8, and they favored this conformation as a solution structure of SyPixD by fluorescence analysis. Similarly, the X-ray structure of AppA by Anderson et al. (*24*) took the Tyr···NH_2 conformation, whereas that by Jung et al. (*25*) and the structure of BlrB (*5*) took the Tyr···O═C conformation. Although the present FTIR data prefer the Tyr···O═C conformation as a solution structure of TePixD, the possibility of the Tyr···NH_2 conformation cannot be excluded at present. The H-bond with the NH_2 of

Gln50 in TePixD could be much stronger than that with the amide NH_2 in a model complex due to, for example, a strong H-bond of the hydrogen of NH_2 to the N5 of flavin. Further DFT calculations for model complexes including the isoalloxazine ring may be necessary to draw a more decisive conclusion about the H-bond partner. It should be emphasized, however, that even in the Tyr···NH_2 conformation Tyr acts as a H-bond donor but not an acceptor.

Upon transition from the dark state to the light state, the νCO frequency upshifted by 8 cm^{-1} from 1265 to 1273 cm^{-1} (Table 1). This upshift was interpreted as due to the strengthened H-bond between the Tyr-OH and Gln (Table 3, Figure 7A). Also, the δCOH change in the opposite direction (a downshift by 7 cm^{-1}; Table 1) suggests that the H-bond angle is also perturbed by the photoreaction. The H-bond angle ($\angle$C−O···O) of Tyr8 in the crystal structure of the dark-state TePixD (*22*) was 108.4°, which is much smaller than the corresponding angles in the optimized structures of model complexes ($\angle$C−O···O = 117.1° for model II and $\angle$C−O···N = 121.4° for model III). This rather distorted H-bond structure in the dark state could be responsible for the relatively high δCOH frequency. This structure may be changed to a stronger H-bond with a proper H-bond angle upon light-state formation. Such changes in the H-bond structure of Tyr8 suggest a significant change in the H-bond network of Tyr8−Gln50−flavin, which is consistent with the formation of a stronger H-bond at the flavin C4═O revealed by a large downshift of the C4═O peak from 1713 to 1698 cm^{-1} (Figure 2) (*7*, *10*, *14*−*21*).

A recent NMR study of AppA by Grinstead at al. (*29*) showed that the proton of Tyr-OH exists in a very stable H-bonding arrangement in the light state, which is in agreement with the strong H-bond interaction of Tyr8 in the light state of TePixD. However, the Tyr-OH resonance was not observed in the NOESY spectrum in the dark state of AppA, and this observation was interpreted as that the Tyr-OH proton exists in a hydrophobic pocket and does not have a H-bonding partner available (*29*). This conclusion is in contrast to the present FTIR results in the dark state of TePixD, in which Tyr8 forms a H-bond most likely to the amide C═O or possibly to the NH_2. It could be possible that the NMR signal was not detected due to a rather weak and distorted H-bond of Tyr-OH in the dark state as suggested in the present FTIR study. Alternatively, the discrepancy could arise from an original conformational difference between TePixD and AppA as has been revealed in the X-ray crystal structures (*22*, *24*).

In conclusion, the present FTIR study provided solid evidence that Tyr8 in TePixD is structurally coupled to the flavin and its H-bond structure is perturbed during photoreaction. The OH of Tyr8 acts as a H-bond donor in both the dark and light states, but the H-bond is strengthened by formation of the light-signaling state concomitant with a change in the H-bond angle. This structural change of Tyr8 may play an important role in the mechanism of photoreaction of the flavin site and subsequent signal transduction in TePixD.

SUPPORTING INFORMATION AVAILABLE

Optimized structures of the model complexes of *p*-cresol that acts as a hydrogen bond donor to the C═O of formamide, *N*-methylformamide, *N*-methylacetamide, diformamide, *N*,*N*-dimethylformamide, and *N*-formylacetamide. This material is available free of charge via the Internet at http://pubs.acs.org.

REFERENCES

1. Van der Horst, M. A., and Hellingwerf, K. J. (2004) Photoreceptor proteins, "star actors of modern times": A review of the functional dynamics in the structure of representative members of six different photoreceptor families, *Acc. Chem. Res. 37*, 13−20.
2. Gomelsky, M., and Klug, G. (2002) BLUF: a novel FAD-binding domain involved in sensory transduction in microorganisms, *Trends Biochem. Sci. 27*, 497−500.
3. Gomelsky, M., and Kaplan, S. (1998) AppA, a redox regulator of photosystem formation in *Rhodobacter sphaeroides* 2.4.1, is a flavoprotein. Identification of a novel fad binding domain, *J. Biol. Chem. 273*, 35319−35325.
4. Masuda, S., and Bauer, C. E. (2002) AppA is a blue light photoreceptor that antirepresses photosynthesis gene expression in *Rhodobacter sphaeroides*, *Cell 110*, 613−623.
5. Jung, A., Domratcheva, T., Tarutina, M., Wu, Q., Ko, W., Shoeman, R. L., Gomelsky, M., Gardner, K. H., and Schlichting, I. (2005) Structure of a bacterial BLUF photoreceptor: Insights into blue light-mediated signal transduction, *Proc. Natl. Acad. Sci. U.S.A. 102*, 12350−12355.
6. Okajima, K., Yoshihara, S., Fukushima, Y., Geng, X., Katayama, M., Higashi, S., Watanabe, M., Sato, S., Tabata, S., Shibata, Y., Itoh, S., and Ikeuchi, M. (2005) Biochemical and functional characterization of BLUF-type flavin-binding proteins of two species of cyanobacteria, *J. Biochem. 137*, 741−750.
7. Okajima, K., Fukushima, Y., Suzuki, H., Kita, A., Ochiai, Y., Katayama, M., Shibata, Y., Miki, K., Noguchi, T., Itoh, S., and Ikeuchi, M. (2006) Fate determination of the flavin photoreceptions in the cyanobacterial blue light receptor TePixD (Tll0078), *J. Mol. Biol. 363*, 10−18.
8. Iseki, M., Matsunaga, S., Murakami, A., Ohno, K., Shiga, K., Yoshida, K., Sugai, M., Takahashi, T., Hori, T., and Watanabe, M. (2002) A blue-light-activated adenylyl cyclase mediates photoavoidance in *Euglena gracilis*, *Nature 415*, 1047−1051.
9. Rajagopal, S., Key, J. M., Purcell, E. B., Boerema, D. J., and Moffat, K. (2004) Purification and initial characterization of a putative blue light-regulated phosphodiesterase from *Escherichia coli*, *Photochem. Photobiol. 80*, 542−547.
10. Laan, W., van der Horst, M. A., van Stokkum, I. H., and Hellingwerf, K. J. (2003) Initial characterization of the primary photochemistry of AppA, a blue-light-using flavin adenine dinucleotide-domain containing transcriptional antirepressor protein from *Rhodobacter sphaeroides*: A key role for reversible intramolecular proton transfer from the flavin adenine dinucleotide chromophore to a conserved tyrosine?, *Photochem. Photobiol. 78*, 290−297.
11. Fukushima, Y., Okajima, K., Shibata, Y., Ikeuchi, M., and Itoh, S. (2005) Primary intermediate in the photocycle of a blue-light sensory BLUF FAD-protein, Tll0078, of *Thermosynechococcus elongatus* BP-1, *Biochemistry 44*, 5149−5158.
12. Ito, S., Murakami, A., Sato, K., Nishina, Y., Shiga, K., Takahashi, T., Higashi, S., Iseki, M., and Watanabe, M. (2005) Photocycle features of heterologously expressed and assembled eukaryotic flavin-binding BLUF domains of photoactivated adenylyl cyclase (PAC), a blue-light receptor in *Euglena gracilis*, *Photochem. Photobiol. Sci. 4*, 762−769.
13. Zirak, P., Penzkofer, A., Schiereis, T., Hegemann, P., Jung, A., and Schlichting, I. (2006) Photodynamics of the small BLUF protein BlrB from *Rhodobacter sphaeroides*, *J. Photochem. Photobiol. B 83*, 180−194.
14. Unno, M., Masuda, S., Ono, T., and Yamauchi, S. (2006) Orientation of a key glutamine residue in the BLUF Domain from AppA revealed by mutagenesis, spectroscopy, and quantum chemical calculations, *J. Am. Chem. Soc. 128*, 5638−5639.
15. Hasegawa, K., Masuda, S., and Ono, T. (2005) Spectroscopic analysis of the dark relaxation process of a photocycle in a sensor of blue light using FAD (BLUF) protein Slr1694 of the cyanobacterium *Synechocystis* sp. PCC6803, *Plant Cell Physiol. 46*, 136−146.
16. Hasegawa, K., Masuda, S., and Ono, T. (2004) Structural intermediate in the photocycle of a BLUF (Sensor of Blue Light

Using FAD) protein Slr1694 in a cyanobacterium *Synechocystis* sp. PCC6803, *Biochemistry 43*, 14979−14986.
17. Hasegawa, K., Masuda, S., and Ono, T. (2006) Light induced structural changes of a full-length protein and its BLUF domain in YcgF(Blrp), a blue-light sensing protein that uses FAD (BLUF), *Biochemistry 45*, 3785−3793.
18. Masuda, S., Hasegawa, K., Ishii, A., and Ono, T. (2004) Light-induced structural changes in a putative blue-light receptor with a novel FAD binding fold sensor of blue-light using FAD (BLUF); Slr1694 of *Synechocystis* sp. PCC6803, *Biochemistry 43*, 5304−5313.
19. Masuda, S., Hasegawa, K., and Ono, T. (2005) Light-induced structural changes of apoprotein and chromophore in the sensor of blue light using FAD (BLUF) domain of AppA for a signaling state, *Biochemistry 44*, 1215−1224.
20. Masuda, S., Hasegawa, K., and Ono, T. (2005) Tryptophan at position 104 is involved in transforming light signal into changes of β-sheet structure for the signaling state in the BLUF domain of AppA, *Plant Cell Physiol. 46*, 1894−1901.
21. Unno, M., Sano, R., Masuda, S., Ono, T., and Yamauchi, S. (2005) Light-induced structural changes in the active site of the BLUF domain in AppA by Raman spectroscopy, *J. Phys. Chem. B 109*, 12620−12626.
22. Kita, A., Okajima, K., Morimoto, Y., Ikeuchi, M., and Miki, K. (2005) Structure of a cyanobacterial BLUF protein, TII0078, containing a novel FAD-binding blue light sensor domain, *J. Mol. Biol. 349*, 1−9.
23. Yuan, H., Anderson, S., Masuda, S., Dragnea, V., Moffat, K., and Bauer, C. (2006) Crystal structures of the *Synechocystis* photoreceptor Slr1694 reveal distinct structural states related to signaling, *Biochemistry 45*, 12687−12694.
24. Anderson, S., Dragnea, V., Masuda, S., Ybe, J., Moffat, K., and Bauer, C. (2005) Structure of a novel photoreceptor, the BLUF domain of AppA from *Rhodobacter sphaeroides*, *Biochemistry 44*, 7998−8005.
25. Jung, A., Reinstein, J., Domratcheva, T., Shoeman, R. L., and Schlichting, I. (2006) Crystal structures of the AppA BLUF domain photoreceptor provide insights into blue light-mediated signal transduction, *J. Mol. Biol. 362*, 717−732.
26. Kraft, B. J., Masuda, S., Kikuchi, J., Dragnea, V., Tollin, G., Zaleski, J. M., and Bauer, C. E. (2003) Spectroscopic and mutational analysis of the blue-light photoreceptor AppA: A novel photocycle involving flavin stacking with an aromatic amino acid, *Biochemistry 42*, 6726−6734.
27. Dragnea, V., Waegele, M., Balascuta, S., Bauer, C., and Dragnea, B. (2005) Time-resolved spectroscopic studies of the AppA blue-light receptor BLUF domain from *Rhodobacter sphaeroides*, *Biochemistry 44*, 15978−15985.
28. Gauden, M., van Stokkum, I. H. M., Key, J. M., Luhrs, D. C., van Grondelle, R., Hegemann, P., and Kennis, J. T. M. (2006) Hydrogen-bond switching through a radical pair mechanism in a flavin-binding photoreceptor, *Proc. Natl. Acad. Sci. U.S.A. 103*, 10895−10900.
29. Grinstead, J. S., Avila-Perez, M., Hellingwerf, K. J., Boelens, R., and Kaptein, R. (2006) Light-induced flipping of a conserved glutamine sidechain and its orientation in the AppA BLUF domain, *J. Am. Chem. Soc. 128*, 15066−15067.
30. Uchida, T., Mogi, T., Nakamura, H., and Kitagawa, T. (2004) Role of Tyr-288 at the dioxygen reduction site of cytochrome *bo* studied by stable isotope labeling and resonance Raman spectroscopy, *J. Biol. Chem. 279*, 53613−53620.
31. Noguchi, T., and Sugiura, M. (2002) Flash-induced FTIR difference spectra of the water oxidizing complex in moderately hydrated photosystem II core films: Effect of hydration extent on S-state transitions, *Biochemistry 41*, 2322−2330.
32. Frisch, M. J., Trucks, G. W., Schlegel, H. B., Scuseria, G. E., Robb, M. A., Cheeseman, J. R., Montgomery, J. A., Jr., Vreven, T., Kudin, K. N., Burant, J. C., Millam, J. M., Iyengar, S. S., Tomasi, J., Barone, V., Mennucci, B., Cossi, M., Scalmani, G., Rega, N., Petersson, G. A., Nakatsuji, H., Hada, M., Ehara, M., Toyota, K., Fukuda, R., Hasegawa, J., Ishida, M., Nakajima, T., Honda, Y., Kitao, O., Nakai, H., Klene, M., Li, X., Knox, J. E., Hratchian, H. P., Cross, J. B., Bakken, V., Adamo, C., Jaramillo, J., Gomperts, R., Stratmann, R. E., Yazyev, O., Austin, A. J., Cammi, R., Pomelli, C., Ochterski, J. W., Ayala, P. Y., Morokuma, K., Voth, G. A., Salvador, P., Dannenberg, J. J., Zakrzewski, V. G., Dapprich, S., Daniels, A. D., Strain, M. C., Farkas, O., Malick, D. K., Rabuck, A. D., Raghavachari, K., Foresman, J. B., Ortiz, J. V., Cui, Q., Baboul, A. G., Clifford, S., Cioslowski, J., Stefanov, B. B., Liu, G., Liashenko, A., Piskorz, P., Komaromi, I., Martin, R. L., Fox, D. J., Keith, T., Al-Laham, M. A., Peng, C. Y., Nanayakkara, A., Challacombe, M., Gill, P. M. W., Johnson, B., Chen, W., Wong, M. W., Gonzalez, C., and Pople, J. A. (2004) Gaussian 03, Revision C.02, Gaussian, Inc., Wallingford, CT.
33. Becke, A. D. (1993) Density-functional thermochemistry. III. The role of exact exchange, *J. Chem. Phys. 98*, 5648−5652.
34. Lee, C., Yang, W., and Parr, R. G. (1988) Development of the Colle-Salvetti correlation-energy formula into a functional of the electron density, *Phys. Rev. B 37*, 785−789.
35. Jakobsen, R. J. (1965) The vibrational spectra of *p*-cresol, *Spectrochim. Acta 21*, 433−442.
36. Takeuchi, H., Watanabe, N., and Harada, I. (1988) Vibrational spectra and normal coordinate analysis of *p*-cresol and its deuterated analogs, *Spectrochim. Acta, Part A 44*, 749−761.
37. Takeuchi, H., Watanabe, N., Satoh, Y., and Harada, I. (1989) Effects of hydrogen bonding on the tyrosine Raman bands in the 1300−1150 cm^{-1} region, *J. Raman Spectrosc. 20*, 233−237.
38. Gerothanassis, I. P., Birlirakis, N., Sakarellos, C., and Marraud, M. (1992) Solvation state of the Tyr side chain in peptides. An FT-IR and ^{17}O NMR approach, *J. Am. Chem. Soc. 114*, 9043−9047.
39. Noguchi, T., Inoue, Y., and Tang, X.-S. (1997) Structural coupling between the oxygen-evolving Mn cluster and a tyrosine residue in photosystem II as revealed by Fourier transform infrared spectroscopy, *Biochemistry 36*, 14705−14711.
40. Hienerwadel, R., Boussac, A., Breton, J., Diner, B. A., and Berthomieu, C. (1997) Fourier transform infrared difference spectroscopy of photosystem II tyrosine D using site-directed mutagenesis and specific isotope labeling, *Biochemistry 36*, 14712−14723.
41. Iwata, T., Nozaki, D., Tokutomi, S., Kagawa, T., Wada, M., and Kandori, H. (2003) Light-induced structural changes in the LOV2 domain of *Adiantum* phytochrome3 studied by low-temperature FTIR and UV-visible spectroscopy, *Biochemistry 42*, 8183−8191.
42. Swartz, T. E., Wenzel, P. J., Corchnoy, S. B., Briggs, W. R., and Bogomolni, R. A. (2002) Vibration spectroscopy reveals light-induced chromophore and protein structural changes in the LOV2 domain of the plant blue-light receptor phototropin 1, *Biochemistry 41*, 7183−7189.
43. Kottke, T., Batschauer, A., Ahmad, M., and Heberle, J. (2006) Blue-light-induced changes in *Arabidopsis* cryptochrome 1 probed by FTIR difference spectroscopy, *Biochemistry 45*, 2472−2479.

BI7004653